




## ARTICLE

## Macrosystems Ecology

## Spatiotemporal variation in the gut microbiomes of co-occurring wild rodent species

Bianca R. P. Brown<sup>1,2,3</sup>  | Leo M. Khasoha<sup>3,4</sup> | Peter Lokeny<sup>3</sup> |  
 Rhiannon P. Jakopak<sup>3,4</sup> | Courtney G. Reed<sup>1,2,3</sup>  | Marissa Dyck<sup>5</sup> |  
 Alois Wambua<sup>4</sup> | Seth D. Newsome<sup>6</sup> | Todd M. Palmer<sup>3,7</sup> |  
 Robert M. Pringle<sup>3,8</sup>  | Jacob R. Goheen<sup>3,4</sup> | Tyler R. Kartzinel<sup>1,2,3</sup>

<sup>1</sup>Department of Ecology, Evolution, and Organismal Biology, Brown University, Providence, Rhode Island, USA

<sup>2</sup>Institute at Brown for Environment and Society, Brown University, Providence, Rhode Island, USA

<sup>3</sup>Mpala Research Centre, Laikipia, Kenya

<sup>4</sup>Department of Zoology and Physiology, University of Wyoming, Laramie, Wyoming, USA

<sup>5</sup>Department of Biological Sciences, Ohio University, Athens, Ohio, USA

<sup>6</sup>Department of Biology, University of New Mexico, Albuquerque, New Mexico, USA

<sup>7</sup>Department of Biology, University of Florida, Gainesville, Florida, USA

<sup>8</sup>Department of Ecology and Evolutionary Biology, Princeton University, Princeton, New Jersey, USA

## Correspondence

Tyler R. Kartzinel

Email: [tyler\\_kartzinel@brown.edu](mailto:tyler_kartzinel@brown.edu)

## Funding information

Institute at Brown for Environment and Society Graduate Research Training Grant, Brown University; University of Wyoming; NSERC; National Science Foundation (Graduate Research Fellowship Program), Grant/Award Numbers: DEB-1547679, DEB-1656527, DEB-1930763, DEB-1930820, DEB-2018405, DEB-2026294, DEB-2132265; Brown University (EEOB Doctoral Dissertation Enhancement Grant)

**Handling Editor:** Rebecca J. Rowe

## Abstract

Mammalian gut microbiomes differ within and among hosts. Hosts that occupy a broad range of environments may exhibit greater spatiotemporal variation in their microbiome than those constrained as specialists to narrower subsets of resources or habitats. This can occur if widespread host encounter a variety of ecological conditions that act to diversify their gut microbiomes and/or if generalized host species tend to form large populations that promote sharing and maintenance of diverse microbes. We studied spatiotemporal variation in the gut microbiomes of three co-occurring rodent species across an environmental gradient in a Kenyan savanna. We hypothesized: (1) the taxonomic, phylogenetic, and functional compositions of gut microbiomes as predicted using the Phylogenetic Investigation of Communities by Reconstruction of Unobserved States (PICRUSt) differ significantly among host species; (2) microbiome richness increases with population size for all host species; and (3) host species exhibit different levels of seasonal change in their gut microbiomes, reflecting different sensitivities to the environment. We evaluated changes in gut microbiome composition according to host species identity, site, and host population size using three years of capture–mark–recapture data and 351 microbiome samples. Host species differed significantly in microbiome composition, though the two species with more specialized diets and higher

This is an open access article under the terms of the [Creative Commons Attribution](https://creativecommons.org/licenses/by/4.0/) License, which permits use, distribution and reproduction in any medium, provided the original work is properly cited.

© 2024 The Authors. *Ecosphere* published by Wiley Periodicals LLC on behalf of The Ecological Society of America.

demographic sensitivities showed only slightly greater microbiome variability than those of a widespread dietary generalist. Total microbiome richness increased significantly with host population size for all species, but only one of the more specialized species also exhibited greater individual-level microbiome richness in large populations. Across co-occurring rodent species with diverse diets and life histories, large host population sizes were associated both with greater population-level microbiome richness (sampling effects) and turnover in the relative abundance of bacterial taxa (environmental effects), but there was no consistent pattern for individual-level richness (individual specialization). Together, our results show that maintenance of large host populations contributes to the maintenance of gut microbiome diversity in wild mammals.

#### KEYWORDS

16S rRNA, capture–mark–recapture, specialization, stable isotopes, symbiosis

## INTRODUCTION

Populations of species capable of utilizing a variety of resources or habitats (i.e., “generalists”) tend to be both widespread and relatively abundant in places where they occur (Brown, 1984). Compared with generalists, specialists tend to have narrower dietary niche breadths, occupy fewer habitats, and maintain smaller population sizes that cumulatively cause their populations to fluctuate as environments change (Brown, 1984). Recently, the mammalian gut microbiome has emerged as a determinant of host nutritional, physiological, and immunological responses to ecological change (Alberdi et al., 2016; Trevelline & Kohl, 2022). Because species may harbor microbiomes that differ in their sensitivity to environmental conditions, anthropogenic impacts on the microbiomes of wildlife could challenge the survival of species that are relatively specialized and/or maintain generally smaller population sizes (Trevelline et al., 2019). Better understanding of how host–microbiome interactions are established and maintained could be a contributing factor in whether and how species survive environmental change (Voolstra & Ziegler, 2020).

External environmental conditions can both directly and indirectly influence gut microbiome diversity. As microbiome diversity reflects the variety of foods that hosts eat and the external environments they occupy, microbiome diversity should theoretically be governed by a balance between two opposing phenomena: intraspecific competition that minimizes the overlap of resource use between host individuals (i.e., promotes individual variation) versus interspecific competition that could promote specialization by constraining variation along one or more niche axes (Araújo et al., 2011; Kernaléguen et al., 2015; Van Valen, 1965). In mammals, external environmental

changes, such as seasonal shifts in temperature or precipitation, may trigger dietary changes that lead to compositionally distinct microbiomes suggestive of a deterministic diet–microbiome linkage (Baniel et al., 2021; Maurice et al., 2015). Nonetheless, host–microbiome associations vary in response to the same ecological changes in ways that complicate predictions (Kartzinel et al., 2019). As specialists may vary less in their extent of dietary change than generalists, it stands to reason that this could constrain microbiome variability such that specialists have less diverse or less variable gut microbiomes through time and space due to their narrower and more constant use of specific resources (Shipley et al., 2009). Conversely, however, if populations of relatively specialized species are generally smaller, more isolated, or otherwise subject to more spatio-temporally variable environments, then stochastic “sampling effects” may enhance microbiome variability through time and space (Levins, 1969; Sharpton, 2018). Identifying how host ecological and demographic variation modifies host–microbiome interactions would improve the understanding of how microbiome diversity is established and maintained (Brown et al., 2023).

There is an expectation that compositionally similar gut microbiomes will respond in qualitatively similar ways as hosts acclimate to similar environmental conditions or respond to similar environmental changes (Amato et al., 2015; Kartzinel et al., 2019; Reese & Dunn, 2018). However, comparative studies of wild host–microbiome interactions tend to focus on species- or population-level differences, such as whether the total or average level of microbiome diversity in a group differs significantly across a set of environmental conditions, and thus may often fail to account for the ways that individuals within a group may vary (Björk et al., 2022). For example, if a pair of populations harbor equivalent total

population-level microbiome diversity, but differ in individual-level microbiome diversity, then the host groups necessarily differ in their levels of among-individual variation. Any individual specialization in the gut microbiome, much like intraspecific feeding specializations and foraging behaviors, could constrain how individuals' ecological interactions vary through space and time (Araújo et al., 2011; Jesmer et al., 2020). Performing microbiome studies only at the level of host population or species can obfuscate crucial variation among individual microbiomes that may be necessary to accurately predict how both groups and individuals respond to change.

Using a comparative time series analysis, we sought to identify how fine-grained spatiotemporal variation influences the microbiomes of three co-occurring rodent species along an environmental gradient in central Kenya: Hinde's bush rat (*Aethomys hindei*), fringe-tailed gerbil (*Gerbilliscus robustus*), and pouched mouse (*Saccostomus mearnsi*). These host species are ideal for comparison because they are relatively abundant and widespread, but they differ in their degrees of omnivory and their demographic sensitivity to environmental change. To characterize variation in microbiome composition according to spatial and environmental conditions, we investigated populations distributed along a sharp north–south rainfall gradient. To characterize spatiotemporal variation in microbiomes within these populations, we investigated associations between rainfall-driven changes in population size and microbiome composition over a three-year study period. We tested three hypotheses: (1) the taxonomic, phylogenetic, and PICRUSt-predicted functional compositions of gut microbiomes differ significantly between host species; (2) individual- and population-level microbiome richness levels would be greatest in large populations of all host species; and (3) host species would differ in the degree of spatiotemporal turnover in the compositional and predicted functional characteristics of their gut microbiomes, reflecting ecological differences in how hosts respond to rainfall-driven environmental change.

## METHODS

### Study site and species descriptions

We conducted our study in a semiarid Kenyan savanna (0°17' N, 37°52' E, 1600-m elevation; Figure 1) within the Ungulate Herbivory Under Rainfall Uncertainty (UHURU) experiment. Located at the Mpala Research Centre, UHURU was established in 2008 (Alston et al., 2022; Goheen et al., 2013, 2018; Kartzin et al., 2014), consisting of three sites (“north,” “central,” and

“south”), separated by 20 km. At each site, there are three blocks containing a 1-ha ungulate exclusion plot that excludes all animals >5 kg and a 1-ha control plot that permits access to all ungulates. Each plot contains a 7 × 7 grid of 49 permanent stakes with 10-m spacing that we use as reference points for vegetation and small mammal surveys. We monitor understory vegetation twice a year (February/March: dry season; October: wet season) using the canopy intercept method, and we survey small mammals every two months for four nights by setting peanut butter baited Sherman traps at each stake. Long-term, over the course of 12 years, understory density has been 3× higher and small mammal richness 7× greater in exclusion plots than in control plots (Alston et al., 2022; Kartzin et al., 2014). From 2015 to 2018 (the course of this study), mean annual precipitation increased from 500 mm/year in the north to 532 mm/year in central, and to 539 mm/year in south, consistent with long-term trends in which both rainfall and plant biomass increase from north to south (Alston et al., 2022). Over the course of our study, mean understory density was greater in the south (549 pin hits per plot) than in the central (328) and north (344) sites (Alston et al., 2022). Historical differences in plant biomass between north and central sites have been converging since 2014, but the south has consistently maintained the highest understory biomass (Alston et al., 2022; Goheen et al., 2013).

### Host populations

Our comparative analysis is based on the three most abundant and widespread rodent species in the UHURU experiment: *S. mearnsi* (Nesomyidae), *A. hindei* (Muridae), and *G. robustus* (Muridae; Alston et al., 2022). We estimated population sizes within each of the 18 study plots (9 ungulate exclusion plots, 9 control) across 17 trapping bouts (2015–2018; Figure 1). Individuals were counted using a capture–mark–recapture method in which rodents were marked with an ear tag upon initial capture (Alston et al., 2022; Brown et al., 2023; Goheen et al., 2013). Population sizes were estimated using capture–mark–recapture data for each species (Alston et al., 2022; Goheen et al., 2013), calculated in a Huggins robust design model framework using RMark in R (Laake, 2013; R Development Core Team, 2021). We summed population size across the three replicate plots of each treatment (i.e., ungulate exclusion or control) within each of the three sites.

For each host species, we compared three measures of demographic and niche variation: population

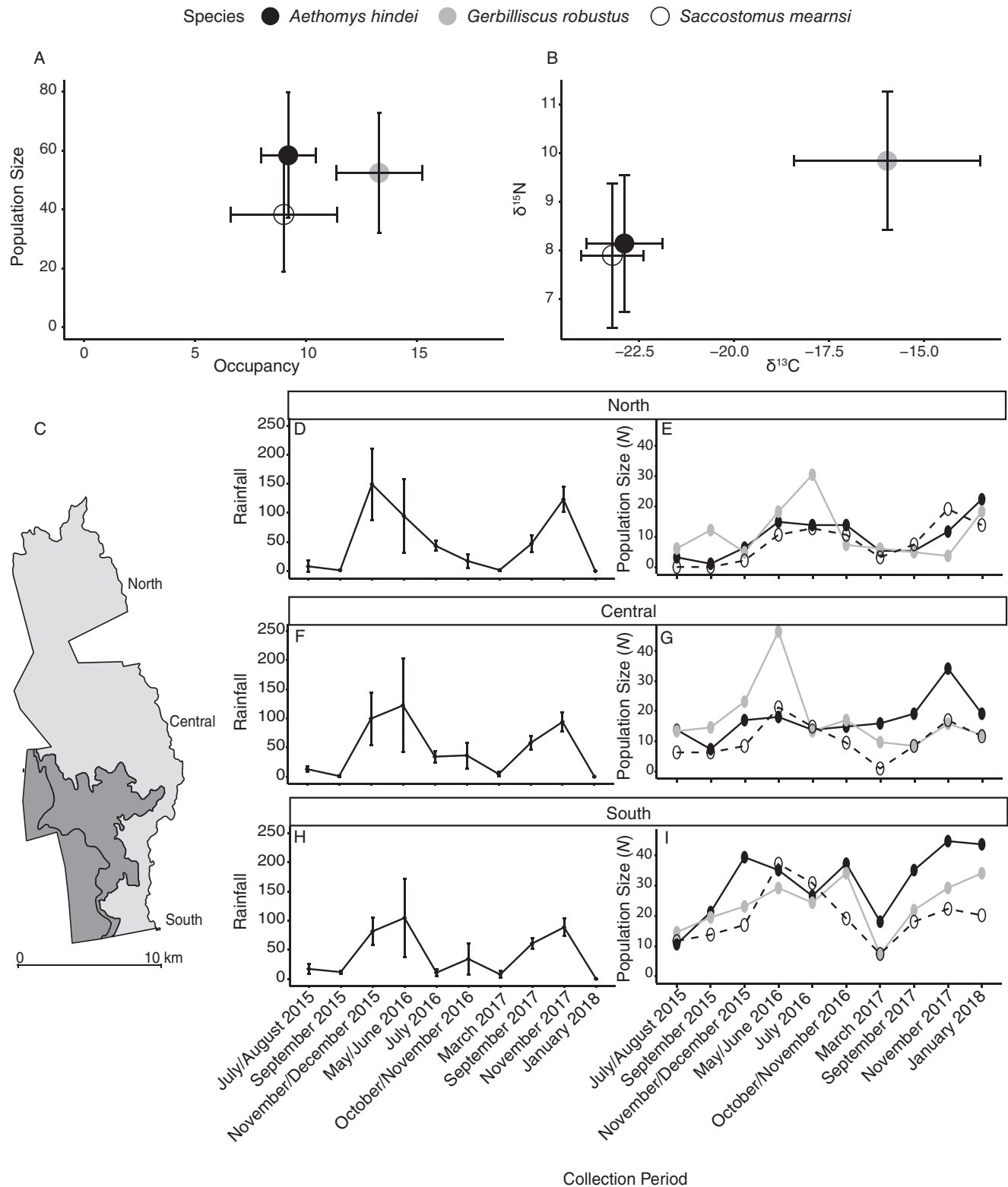


**FIGURE 1** Spatiotemporal variation in host population size, distribution, and resource use with respect to variation in rainfall. (A) Comparison of mean population size and site occupancy of the three host species through time, with bars representing SE. (B) Carbon ( $\delta^{13}\text{C}$ ) and Nitrogen ( $\delta^{15}\text{N}$ ) isotope values of host species included in our analysis. (C) Map of Mpala Research Centre showing the three study sites (north, central, and south). (D–F) The mean 30-day cumulative rainfall across each of the three replicate study plots across each of the three sites revealed similar timing of seasonal variation. (E–G) The population sizes of each host species at each site were estimated using RMark based on the total capture history of individuals across the three replicate plots at each site. We quantified spatiotemporal correlations between each of these aspects of host ecology (and their coefficients of variation; Appendix S1: Figure S1).

abundance (population size per site and, hence, population density), occupancy (the number of plots in which each species was trapped in each sampling bout, out of all 18 plots), and the extent to which species' diets overlapped based on blood plasma carbon ( $\delta^{13}\text{C}$ ) and nitrogen ( $\delta^{15}\text{N}$ ) stable isotopes values. To compare seasonal variation in abundance and occupancy, we calculated the coefficient of variation of population size and plot occupancy across repeated trapping bouts (Appendix S1: Figure S1). To compare  $\delta^{13}\text{C}$  and  $\delta^{15}\text{N}$  isotope values, data generated in a prior study that considered species-level variation in resource use from these and other host species in this same study system were used (Brown et al., 2023). Briefly, we used a Costech 4010 elemental analyzer coupled with a (1) Thermo Finnigan Delta plus XP isotope ratio mass spectrometer at the University of Wyoming Stable Isotope Facility (Laramie, WY), or (2) Thermo Fisher Delta V isotope ratio mass spectrometer at the University of New Mexico Centre for Stable Isotopes (Albuquerque, NM). Isotope data were reported as  $\delta^{13}\text{C}$  or  $\delta^{15}\text{N} = 1000 \times ([R_{\text{sample}} - R_{\text{standard}}] / R_{\text{standard}} - 1)$ , where  $R_{\text{sample}}$  and  $R_{\text{standard}}$  are the  $^{13}\text{C}/^{12}\text{C}$  or  $^{15}\text{N}/^{14}\text{N}$  ratio of samples and standards, respectively. Laboratory reference materials were calibrated to the internationally accepted standards Vienna Pee Dee Belemnite limestone (V-PDB) and atmospheric nitrogen (AIR), respectively, with units expressed in parts per thousand (‰). Analytical precision was calculated as the mean within-run SD of reference materials, which was  $\pm 0.2\text{‰}$  for both  $\delta^{13}\text{C}$  and  $\delta^{15}\text{N}$  values. These data showed that *A. hindei* and *S. mearnsi* were relatively specialized on  $\text{C}_3$  vegetation compared with *G. robustus*, which consumed a comparatively broad mixture of  $\text{C}_3$  and  $\text{C}_4$  vegetation and exhibits more omnivory (Figure 1; Appendix S1: Figure S1; Brown et al., 2023). We tested for significant differences between host species in all host demographic and dietary metrics using ANOVA followed by Tukey's honestly significant difference test.

To identify links between rainfall and resource availability, we investigated cross-correlations between rainfall, population size, and population growth rate. We found moderate to strong correlations between population growth rate and population size in each site-treatment combination of plots and across all host species at each bout during the study period (Appendix S1: Figure S2). The positive correlations between the estimated population sizes and corresponding population growth rates indicated that we sampled large populations when they tended to have experienced recent population growth, whereas we sampled small populations when they tended to have recently experienced population decline (Appendix S1: Figure S2). Correlations confirmed that

relatively high levels of recent rainfall were correlated with relatively large population sizes, such that the largest populations tended to be sampled from more mesic sites following seasonal precipitation (Appendix S1: Figure S2). We therefore chose to use population size as an informative ecological predictor of the combined effects that seasonal variation in the local environment (i.e., rainfall, habitat characteristics, resource availability, predation risk) and the local host population (i.e., population size, growth rate, density, social interactions) may have on the richness and composition of gut microbiomes.

## Microbiome sample collection

We collected fecal (gut) microbiome samples during a subset of 10 sampling bouts between July 2015 and January 2018 (Figure 1; see tab. S1 in Dryad Repository; Brown et al., 2024). Whenever possible, we collected fecal samples directly from animals captured in Sherman traps by allowing them to defecate into disposable plastic bags. If an animal did not defecate and a fresh fecal sample was available in the trap, we collected that sample for analysis. To reduce cross-contamination of fecal samples between animals caught on different nights, we removed fecal pellets and food from traps daily, and traps were washed with detergent between bouts. To preserve fecal DNA, we transferred fecal samples to lysis tubes containing Zymo Xpedition buffer and homogenized the sample by vortexing for at least 30 s before freezing it. To extract DNA, we used Zymo Soil/Fecal mini kits in a laboratory that included separate pre- and post-PCR rooms and equipment. To monitor for contamination, we included an extraction blank treated identically to fecal samples; this blank, which did not contain any sample, was included whenever we performed extractions.

## Microbiome sequencing and analysis

We used amplicon sequencing of bacterial 16S rRNA to profile gut microbiomes in our study. We generated amplicons of the V4-hypervariable region of 16S using primers 515f and 806r (Walters et al., 2016). Amplicons were normalized in concentration, pooled, quality checked using Qubit and Bioanalyzer, and then sequenced on a  $2 \times 250$  bp paired-end Illumina MiSeq run using a v2 500-cycle reagent cartridge. In addition to amplicons from fecal DNA, we sequenced the amplicons of extraction blanks and PCR controls to evaluate accuracy and screen the resulting data for potential



contaminants. In total, we obtained data from 351 fecal samples in addition to PCR-negative controls ( $N = 5$ ), PCR-positive controls (ZymoBIOMICS Microbial Communities, No. D6305;  $N = 5$ ), and extraction blanks ( $N = 8$ ). Our 351 microbiome samples represented 25–52 samples per site per species through time (median = 40), 291 (83%) of which were obtained from unique individuals and 59 of which were from 28 individuals that were sampled two to four times during the study period. A total of 45,238,720 Illumina sequence reads were obtained prior to filtering (median = 120,338 per sample).

Our strategy to generate data on the relative abundance of bacterial taxa included bioinformatic processing and taxonomic assignments of amplicon sequence variants (ASVs). We removed primer sequences and truncated reads to 213 bp using DADA2 (Callahan et al., 2016) in R. We ran the DADA2 sequence-variant algorithm (i.e., dadaFs/Rs) on dereplicated sequences with their assigned error rates before merging forward and reverse sequence reads into ASVs. We then assigned taxonomy to resulting ASVs by comparing them to SILVA version 132 (Quast et al., 2013) using the Bayesian algorithm in QIIME2 (Bokulich et al., 2018; Thompson et al., 2017). We screened for potential contaminants by comparing observed and expected ASVs in the mock community samples and removed them from all samples prior to further analysis (Brown et al., 2023). After filtering ASVs to remove contaminants, mitochondria, chloroplasts, and taxa other than bacteria (Eukarya and Archaea), the dataset retained 23,606,045 sequences (median = 64,720 per sample) representing a total of 12,770 ASVs. We constructed a bacterial phylogeny tree to calculate UniFrac distances by aligning ASVs using MAFFT (Kato, 2002) then building the phylogeny using FastTree (Price et al., 2009) in QIIME2. To enable microbiome diversity and composition comparisons, we rarefied samples to a depth equal to the sample with the fewest remaining reads ( $N = 11,501$  reads/sample) producing a final dataset that contained 11,055 ASVs (Appendix S1: Figure S3).

We quantified taxonomic, phylogenetic, and predicted functional differences in host microbiomes. We calculated taxonomic differences using Bray–Curtis dissimilarity and calculated phylogenetic differences using weighted and unweighted UniFrac metrics (weighted considers the relative abundance of each ASV; unweighted considers only presence/absence of each ASV). We predicted functional variation among microbiomes using PICRUST2 (Douglas et al., 2020). To construct a PICRUST2 dataset, we aligned ASVs to a reference tree consisting of marker genes from 41,926 known archaeal and bacterial genomes that were

dereplicated to 20,000 16S rRNA gene clusters. Based on the abundance of each ASV in each sample, the gene family copy numbers were used to calculate MetaCyc pathway abundances. We added the corresponding MetaCyc functional descriptions and rarefied the resulting pathway abundance table to the lowest number of pathways per sample. We used the resulting dataset to calculate pairwise Bray–Curtis dissimilarity of PICRUST2-predicted functional characteristics of bacteria between samples.

We quantified microbiome richness at both the individual and population levels. Individual-level richness was calculated as the total number of ASVs per sample. To quantify total population-level richness, we used sample-based rarefaction using samples collected during each sampling bout at each site for which we obtained microbiome data from three or more individuals using interpolation and extrapolation (iNEXT; Hsieh et al., 2016). We performed a sample-based rarefaction using the bacterial richness value from samples collected during each bout at each of the three sites when microbiome data were available for three or more samples. To facilitate comparison of bouts and sites for which we obtained different numbers of samples, we based comparisons on species-accumulation curves at values equivalent to nine samples per site. The output from this analysis provided a single population-level bacterial richness value for each species at each location during each bout.

## Hypothesis testing

To test Hypothesis 1, which was that microbiomes consistently differed among host species in taxonomic, phylogenetic, and functional compositions, we evaluated variation in the (1) Bray–Curtis taxonomic dissimilarity, (2) unweighted UniFrac, (3) weighted UniFrac, and (4) PICRUST2-predicted functional dissimilarity among all samples. We tested for significant differences among host species using both global and pairwise permutational multivariate analysis of variance (PERMANOVA) with 999 permutations in vegan (Anderson & Walsh, 2013; Martinez Arbizu, 2017; Oksanen et al., 2017). Bout was included as a random effect in all models. We also tested for significant differences in interindividual variation using a multivariate homogeneity of group dispersion analysis using betadisper in vegan, with 999 permutations. To visualize microbiome variation across the four metrics, we performed principal coordinate analysis (PCoA). We performed differential abundance analysis of predicted functional pathways between host species using Songbird, which quantifies the log ratios of predicted microbial functions within host groups

(Morton et al., 2019). We selected the top 10 predicted functional pathways from each pairwise comparison of host species and performed a Wilcoxon test to test whether the magnitude of log ratios for these pathways was significantly different between pairs. A significant difference would suggest that one species has stronger seasonal associations with its top 10 predicted functional pathways than the other. To facilitate further comparisons of spatiotemporal variation in microbiome composition among host species, we then subset our data to include only samples from the ungulate exclusion plots of the UHURU experiment for comparative analyses because all three host species were regularly trapped and sampled from this subset of plots, enabling both intra- and interspecific comparisons through time and across sites (i.e., north, central, south; Table 1; Alston et al., 2022).

To test our second hypothesis (that spatiotemporal variation in population size is correlated with microbiome richness), we focused on samples collected from the exclusion plots ( $N = 294$ ) and compared microbiome richness at two scales: (1) fecal samples from individuals, and (2) total population-level richness

whenever  $\geq 3$  samples were available to enable reliable estimation at each site and bout. At each scale, we performed linear mixed modeling with microbiome richness as the response variable and model predictors that included population size, site, and the population size  $\times$  site interaction, with collection bout representing a random intercept to account for repeated sampling of populations through time, in the package lme4 in R (Bates et al., 2015).

We tested our third hypothesis (that host species would differ in their degree of spatiotemporal variation in microbiome composition) by investigating population size and site as drivers of microbiome variation among samples collected from exclusion plots ( $N = 294$ ). For each host species, we investigated spatiotemporal variation in microbiome composition using PERMANOVA and dispersion analyses involving all four compositional metrics: (1) Bray–Curtis, (2) unweighted, and (3) weighted UniFrac metrics, and (4) predicted functional differences based on PICRUSt2. Our PERMANOVAs evaluated variation based on population size, site, and the population  $\times$  site interaction with 999 permutations. Bout was included as a random effect for all models. Our

**TABLE 1** Microbiome sampling and richness data.

Species	Site	Treatment	Population size			Individual richness		Population richness	
			Mean	SD	<i>N</i>	Mean	SD	Mean	SD
<i>Aethomys hindei</i>	North	Control	0	0	0				
	North	Exclusion	10	7	34	421	98	2012	154
	Central	Control	1	1	1	493			
	Central	Exclusion	17	7	32	481	122	2007	276
	South	Control	1	1	1	743			
	South	Exclusion	31	11	39	513	114	2394	317
<i>Gerbilliscus robustus</i>	North	Control	3	3	12	473	100	1835	
	North	Exclusion	9	7	30	478	144	2015	227
	Central	Control	6	6	24	451	117	1884	123
	Central	Exclusion	11	5	28	440	108	1670	257
	South	Control	6	4	10	471	86	1869	0
	South	Exclusion	18	8	34	470	111	2140	408
<i>Saccostomus mearnsi</i>	North	Control	0	0	0				
	North	Exclusion	8	7	25	518	118	1682	461
	Central	Control	0	1	2	454	74		
	Central	Exclusion	10	6	37	514	113	2058	222
	South	Control	2	2	7	494	153		
	South	Exclusion	17	9	35	524	147	2146	361

*Note:* For each host species, site, and treatment combination, we report the mean host population size with SD, the number of samples analyzed (*N*), the mean ASV richness per sample per bout with SD, and the mean population-level ASV richness per bout with SD. Averages were calculated when  $N > 1$ ; totals when  $N > 2$ .

Abbreviation: ASV, amplicon sequence variant.

analyses of interindividual variation within each host species involved calculating the distance of each sample to the multivariate centroid of the points representing each species' microbiome using betadisper. We then performed linear mixed modeling using this centroid distance as the response variable together with population size, site, and population size  $\times$  site interaction as predictor variables and sampling bout as a random intercept.

To identify bacterial ASVs that may have contributed strongly to the overall patterns of spatiotemporal variation in the microbiomes of each host species, and to compare the strength of spatiotemporal turnover in ASVs within host populations, we used multinomial regression to identify ASVs associated with high or low population densities across sites. We conducted this analysis by defining categorical groupings of high and low host population sizes for each host species at each site. The high and low categories were based on the median population size of each host species at each site: *A. hindei* (north 14; central 18; south 35), *G. robustus* (13; 11; 20), and *S. mearnsi* (11; 10; 16). Using the multinomial regression method implemented in Songbird (Morton et al., 2019), we identified the log-fold ratio of ASVs between periods of high and low population size at each site for each species. The log ratio was used to rank ASVs from the most to least sensitive to changes in population size. The regression model utilized unrarefied ASV count data after removing ASVs that were present in <0.1% of samples. We ran separate models for each host species at each site with a differential prior of 0.5 and 10,000 epochs. We identified the top 10 differentially ranked ASVs associated with both high and low population sizes as the most sensitive to changes in population size (Morton et al., 2019). We tested for significant differences in the magnitude of the log ratios of the top 10 ASVs between high and low population sizes at each site for each species using Wilcoxon tests.

## RESULTS

### Host ecology

We compared host species based on demographic and dietary sensitivities to spatiotemporal variation. The average population size for *A. hindei* was 1.5-fold greater than that for *S. mearnsi*. The average population size of *G. robustus* was intermediate between the two (Table 1; Figure 1; Appendix S1: Figure S1). The coefficient of variation for population size through time did not differ significantly between *A. hindei* and *S. mearnsi*, which both had values that were approximately 1.7-fold greater than for *G. robustus* (Appendix S1: Figure S1). Throughout the

study period, *G. robustus* occupied an average of 13 plots; *A. hindei* and *S. mearnsi* both occupied an average of 9 out of 18 plots (Figure 1; Appendix S1: Figure S1; see tab. S2 in Dryad Repository; Brown et al., 2024). Both *A. hindei* and *S. mearnsi* had broadly overlapping dietary niches, with low and overlapping  $\delta^{15}\text{N}$  and  $\delta^{13}\text{C}$  values indicative of a plant-based diet and similar consumption of  $\text{C}_4$ -grasses in their primarily  $\text{C}_3$ -plant diets (Figure 1; Appendix S1: Figure S1). In contrast, *G. robustus* exhibited a wider dietary breadth, with  $\delta^{13}\text{C}$  indicative of diets incorporating a mixture of  $\text{C}_3$  and  $\text{C}_4$  plants, and higher  $\delta^{15}\text{N}$  values that suggest a greater degree of trophic omnivory (Figure 1; Appendix S1: Figure S1). In sum, *S. mearnsi* and *A. hindei* populations were more sensitive to rainfall than *G. robustus*, which had a relatively generalized omnivorous diet and less variability in population size (Appendix S1: Figure S1).

### Microbiome data

The relative read abundance (RRA) of microbiome sequences reflected a predominance of Firmicutes and Bacteroidetes for *A. hindei* (mean =  $60\% \pm 0.10$  and  $28\% \pm 0.08$  per sample, respectively), *G. robustus* ( $55\% \pm 0.12$  and  $32\% \pm 0.10$ ), and *S. mearnsi* ( $66\% \pm 0.09$  and  $25\% \pm 0.08$ ). Out of all ASVs, a total of 10,173 (92%) were assigned to a pathway using PICRUSt2, and these reflected at least 292 predicted pathways based on the MetaCyc database. The weighted Nearest Sequenced Taxon Index (NSTI), which measures the phylogenetic distance of an ASV to the reference genomes available for functional analysis, was similar across datasets from all three host species and facilitated pairwise comparisons (*A. hindei* mean = 0.1, range = 0.1–0.2,  $\pm 0.02$  SD; *G. robustus* mean = 0.1, range = 0.1–0.2,  $\pm 0.02$  SD; *S. mearnsi* mean = 0.1, range = 0.06–0.2,  $\pm 0.02$  SD). Each of the remaining 19 bacterial phyla represented a mean of <5% RRA per sample across all host species (Appendix S1: Figure S4). Pairwise comparison of the top 10 predicted functional pathways between host species showed that the gut microbiome of *G. robustus*, the widespread omnivore, had substantially more predicted functional dissimilarity to the microbiomes of both other host species than did comparisons between the microbiomes of these two relatively specialized herbivores (Appendix S1: Figure S5). Similar sets of predicted pathways were enriched in the microbiomes of these two herbivores when compared with *G. robustus*: carbohydrate biosynthesis, isopropanol biosynthesis, and aromatic compound degradation (Appendix S1: Figure S5). Amino acid degradation pathways were more enriched in *G. robustus* when compared with the two herbivores and



represented 4 of the top 10 enriched pathways when compared with *A. hindei* and *S. mearnsi*. When the predicted functional pathways of microbiomes in the two herbivores were compared, amino acid and aromatic compound degradation pathways were enriched in *S. mearnsi* (suggesting a diet with more plant secondary defense compounds), while carbohydrate biosynthesis and inorganic nutrient metabolism were enriched in *A. hindei* (suggesting a diet with more readily available glucose; Appendix S1: Figure S5).

## Hypothesis testing

Consistent with our first hypothesis, each host species exhibited strong and significant differences in microbiome composition based on all four metrics (Figure 2). The weighted UniFrac metric that accounts for variation in the relative abundance of bacterial lineages revealed significant, yet slightly weaker differences in microbiome composition compared with the other taxonomic and phylogenetic metrics, indicating broadly similar ratios of major bacterial lineages in each species' microbiome (i.e., predominance of Firmicutes and Bacteroidetes; Figure 2; Appendix S1: Figure S4). At a finer taxonomic grain, however, the Bray–Curtis dissimilarity of ASVs and unweighted UniFrac revealed strikingly different gut microbiomes among all host species (Figure 2). For both Bray–Curtis dissimilarity and unweighted UniFrac, the two herbivorous species, *A. hindei* and *S. mearnsi*, had more similar microbiomes to each other than to the omnivore *G. robustus* (measuring 1%–3% more similar, depending on metric, and clustering to the left along PCoA Axis 1; Figure 2A–C; see tab. S15 in Dryad Repository; Brown et al., 2024). Species identity also explained significant variation in the predicted functional pathways of each host species' microbiome, and the first two axes of the PCoA accounted for a relatively high % of variation compared with other metrics (Figure 2G). Specifically, the two herbivorous species had more similar predicted function profiles to each other (mean Bray–Curtis dissimilarity = 0.09) than to the omnivorous *G. robustus* (mean Bray–Curtis dissimilarity = 0.11 vs. *A. hindei*; 0.12 vs. *S. mearnsi*; see tab. S16 in Dryad Repository; Brown et al., 2024). Yet, while the extent of interindividual variation in gut microbiome composition differed among host species based on the identities of bacterial taxa they included, there was no difference in the degree of interindividual variation of predicted functional pathways among host species (Figure 2H). Thus, despite hosting similar lineages of gut bacteria (Figure 2; Appendix S1: Figure S4), these co-occurring rodent

species exhibited fine-grained differences in the taxonomic and predicted functional composition of their microbiomes—all of this diversity was distributed broadly among hosts within species.

Consistent with our second hypothesis, there was a significant and positive correlation between host population size and population-level microbiome richness (Figure 3). At the population level, microbiome richness varied significantly with population size, site, and the population size  $\times$  site interaction for all three host species (Figure 3A–C). However, there was no strong or consistent correlation between the richness of individual microbiome samples and population size or site (Figure 3D–F). Only *A. hindei* exhibited the predicted significant overall increase in individual-level microbiome richness with population size, but this pattern was complicated by a population size  $\times$  site interaction in which individual microbiome richness declined with population size at the xeric northern site (there was a similar, but not statistically significant interaction for the generalist *G. robustus*; Figure 3D–F). Larger populations thus collectively harbored more gut bacterial ASVs in all three host species, but the proportion of these ASVs that were held within individuals varied.

Results did not generally support our third hypothesis, that host species would differ in the degree of turnover in their gut microbiomes in ways that reflect differences in host sensitivity to environmental change. Both *A. hindei* and *S. mearnsi* exhibited substantial variation in site occupancy due to environmental variation as well as more specialized diets than the widespread generalist *G. robustus* (Figure 1), but their microbiomes did not exhibit an obviously greater degree of spatiotemporal variability (Figure 4; Tables 2 and 3; Appendix S1: Figure S6). The more environmentally sensitive species, *A. hindei* and *S. mearnsi*, and the generalist species, *G. robustus*, exhibited idiosyncratic patterns in all four metrics of microbiome composition according to variation in population size, site, and the population size  $\times$  site interaction (Figure 4; Tables 2 and 3). There were significant differences in microbiome composition according to population size across all taxonomic and phylogenetic metrics for *A. hindei*, but no significant differences in predicted functional pathways (Figure 4; Tables 2 and 3). In contrast, *S. mearnsi* exhibited significant differences in microbiome composition according to population size based on Bray–Curtis, and unweighted UniFrac and *G. robustus* exhibited significant differences only in taxonomic composition measured by Bray–Curtis according to population size (Figure 4; Tables 2 and 3). The relative abundance of the top 10 most responsive bacterial ASVs to changes between high and low population sizes revealed similar log-fold magnitudes of change for all

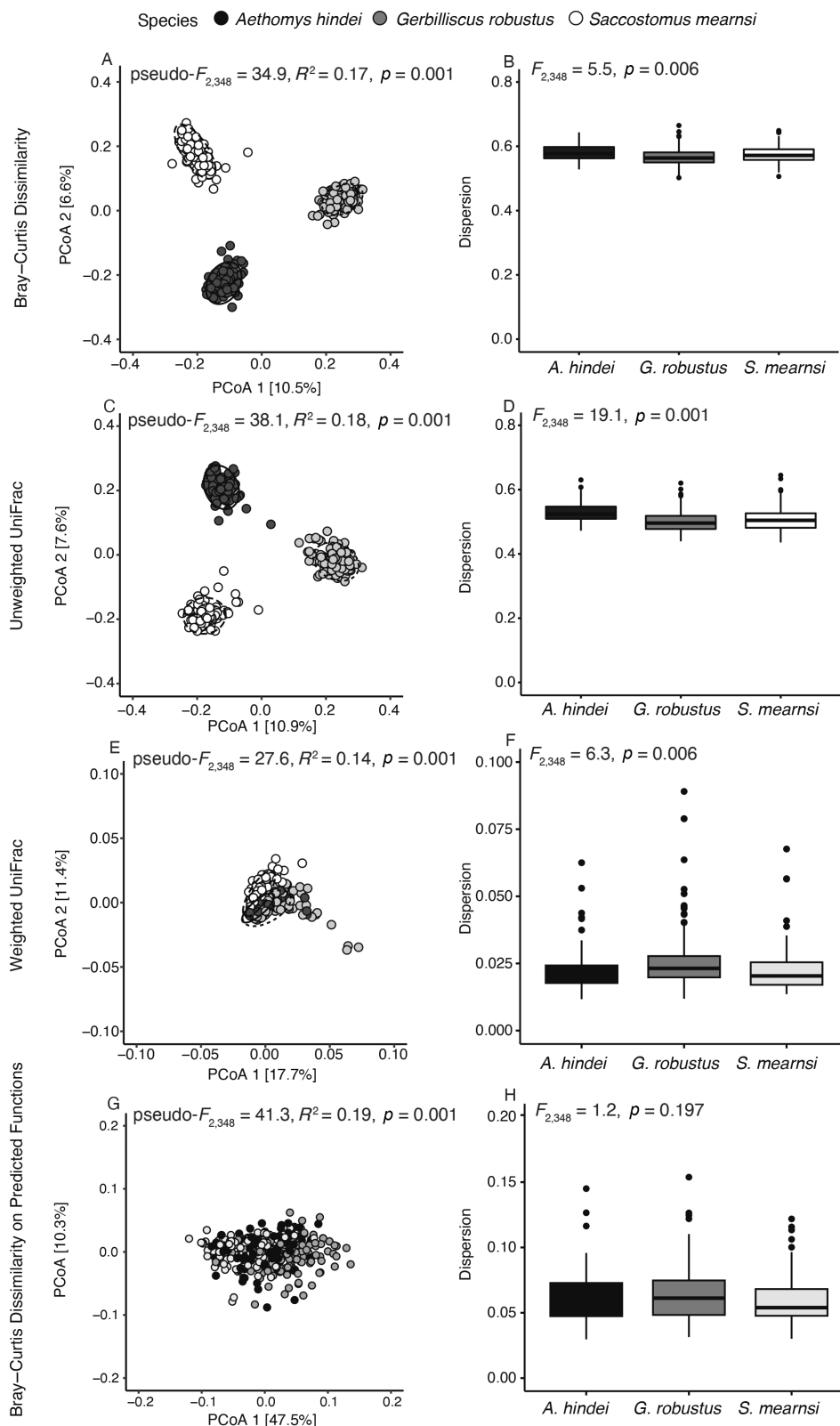


**FIGURE 2** Taxonomic, phylogenetic, and predicted functional variation in microbiomes of each host species. Principal coordinate analyses (PCoAs; left) and dispersion analyses (right) are presented for (A, B) Bray–Curtis dissimilarity, (C, D) unweighted and (E, F) weighted UniFrac metrics, and (G, H) Phylogenetic Investigation of Communities by Reconstruction of Unobserved States (PICRUST)-predicted functional pathways. Ordination axes are labeled according to the % variation they represent. Significant differences in composition among host species were evaluated using permutational multivariate analysis of variances, which are reported in standard notation to include pseudo- $F$  values, df,  $R^2$  values, and  $p$  values. Boxplots show interindividual dispersion values for each host species: central lines represent medians; upper and lower whiskers show inter-quartile ranges; points are outliers. Significant differences in dispersion among host species were evaluated by ANOVAs, which are reported in standard notation to include  $F$  values, df, and  $p$  values.

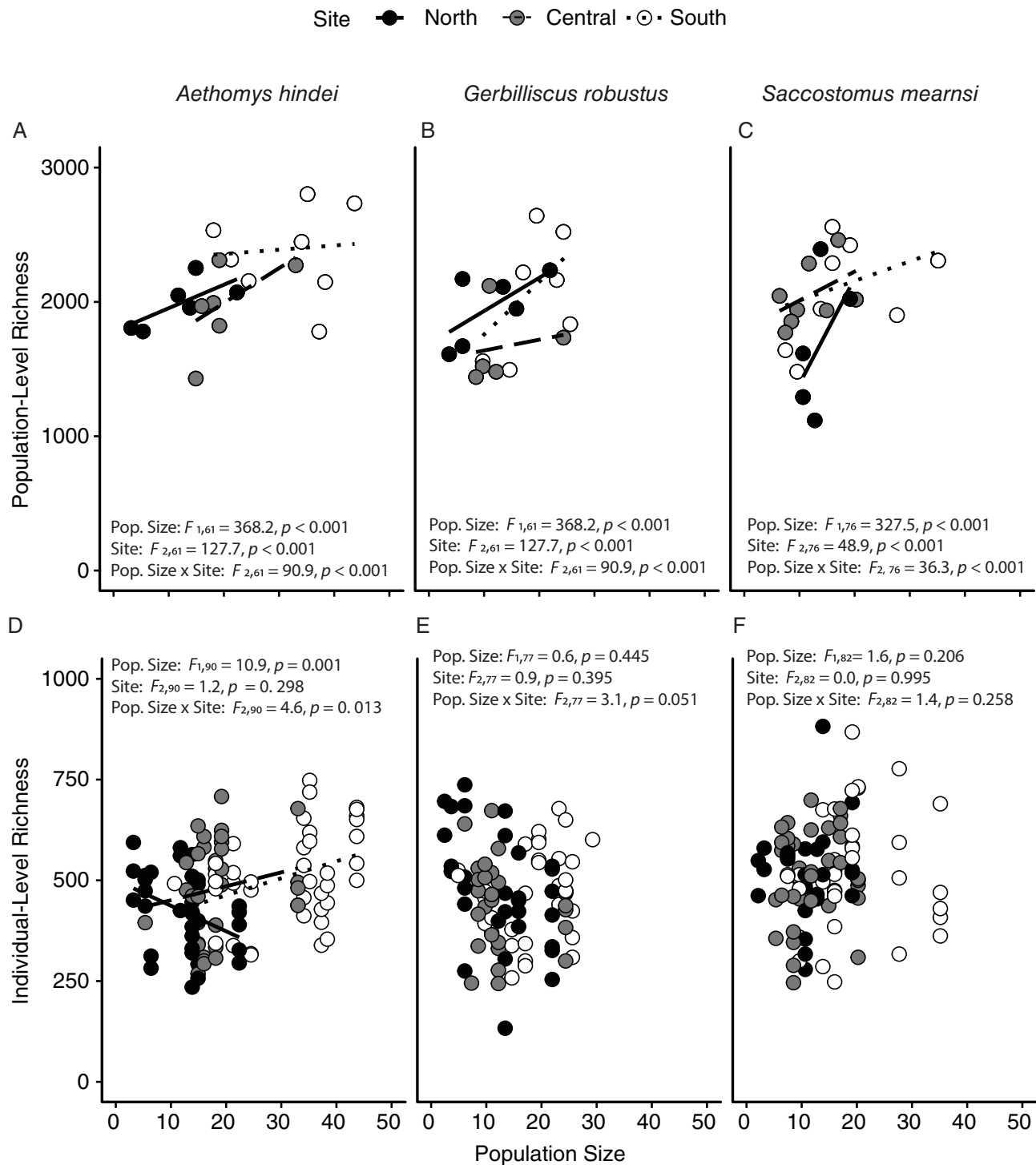


**FIGURE 3** Spatiotemporal variation in microbiome richness across host species. Correlations show (A–C) total population-level microbiome richness and (D–F) individual-level microbiome richness as a function of population (“pop.”) size, site, and the population size × site interaction. Sampling bout was included as a random effect in the models. Separate lines are fit for the north, central, and south sites for all comparisons with significant differences (A–D).

three species (Appendix S1: Figures S7–S9). The bacterial taxa that were most sensitive to population size varied across sites and host species: each host species showed differentially abundant ASVs belonging to the phyla Bacteroidetes, Firmicutes, Tenericutes, and Verrucomicrobia, but *A. hindei*

and *S. mearnsi* were the only species to harbor especially sensitive ASVs belonging to the phylum Actinobacteria (Appendix S1: Figures S7–S9). The spatiotemporally sensitive Actinobacteria associated with *A. hindei* belonged to a different order (Coriobacteriales) than those associated with

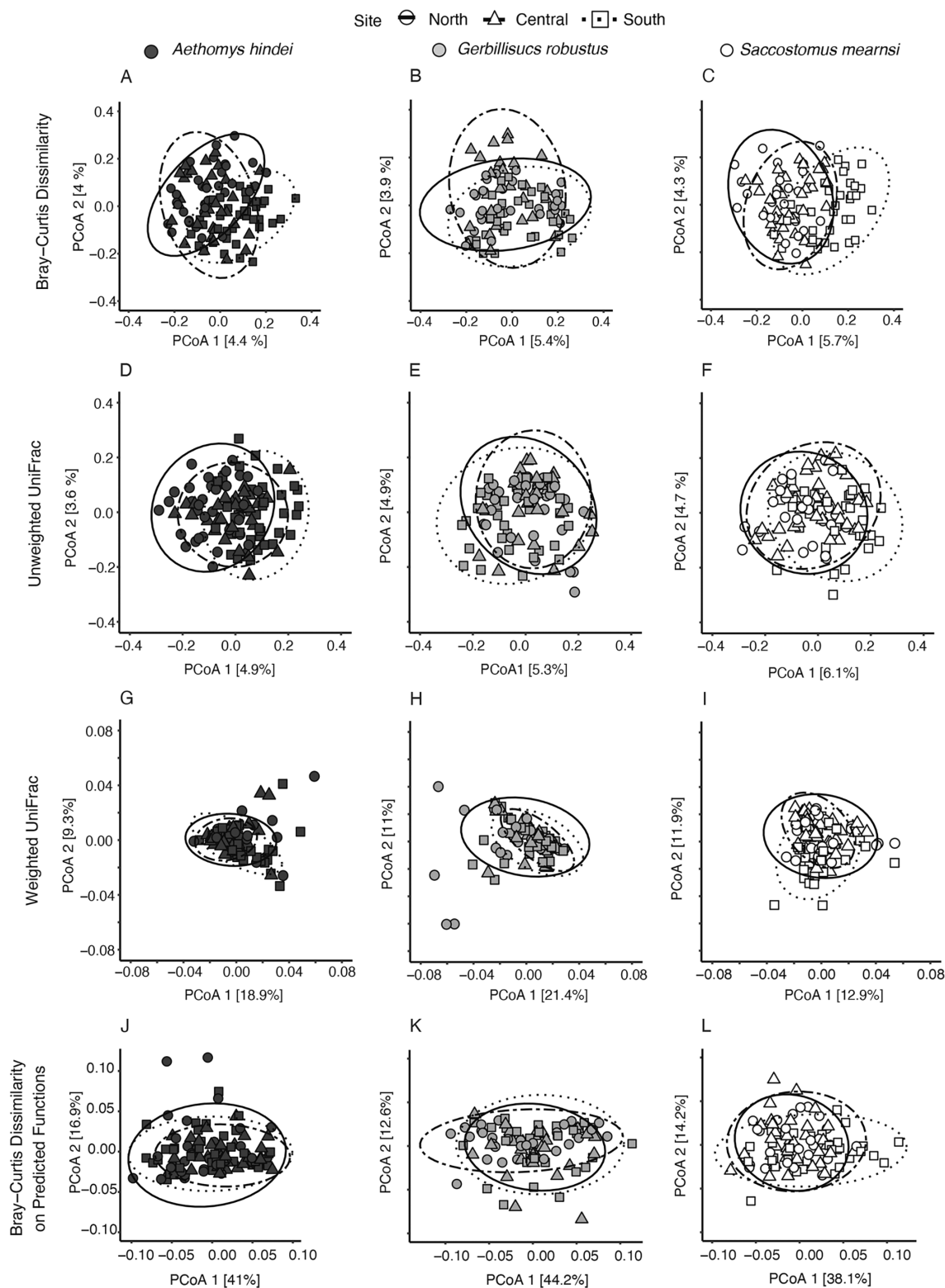


**FIGURE 4** Spatiotemporal variation in microbiome composition by host species. Principal coordinate analyses (PCoAs) ordinations of microbiome data from each host species show (A–C) Bray–Curtis dissimilarity of bacterial ASVs, (D–F) unweighted UniFrac, (G–I) weighted UniFrac, and (J–L) Bray–Curtis dissimilarity of Phylogenetic Investigation of Communities by Reconstruction of Unobserved States (PICRUST)-predicted functional pathways. Ordination axes are labeled according to the percentage of variation they represent. Host species are arranged in columns: *A. hindei* (left), *G. robustus* (center), and *S. mearnsi* (right). Different point shapes denote each of the three study sites (i.e., north, central, and south), with 95% confidence ellipses. Corresponding permutational multivariate analysis of variance (PERMANOVA) results are shown in Tables 2 and 3, and analyses of dispersion are shown in Appendix S1: Figure S6.

**TABLE 2** Permutational multivariate analysis of variance (PERMANOVA) testing the effects of population size, site, and the population size  $\times$  site interaction on microbiome community measured using Bray–Curtis dissimilarity and unweighted and weighted UniFrac distances.

Variable	df	Bray–Curtis			Unweighted UniFrac			Weighted UniFrac		
		Pseudo- <i>F</i>	<i>R</i> <sup>2</sup>	<i>p</i>	Pseudo- <i>F</i>	<i>R</i> <sup>2</sup>	<i>p</i>	Pseudo- <i>F</i>	<i>R</i> <sup>2</sup>	<i>p</i>
<i>Aethomys hindei</i>										
Population size	1	2.4	0.02	0.001	2.3	0.02	0.001	2.6	0.02	0.002
Site	2	1.9	0.04	0.001	1.9	0.03	0.001	1.7	0.03	0.017
Population size × site	2	1.2	0.02	0.023	1.2	0.02	0.003	1.4	0.03	0.125
Residual	99		0.92			0.92			0.92	
Total	104		1			1			1	
<i>Gerbilliscus robustus</i>										
Population size	1	1.3	0.01	0.039	1.2	0.01	0.099	0.9	0.01	0.664
Site	2	2.2	0.05	0.001	2.3	0.05	0.001	2.7	0.06	0.001
Population size × site	2	1.5	0.03	0.002	1.5	0.03	0.003	1.7	0.04	0.124
Residual	86		0.91			0.91			0.9	
Total	91		1			1			1	
<i>Saccostomus mearnsi</i>										
Population size	1	1.7	0.02	0.015	2.0	0.02	0.001	1.7	0.02	0.221
Site	2	3.1	0.06	0.001	3.1	0.06	0.001	3.1	0.06	0.001
Population size × site	2	1.3	0.03	0.009	1.1	0.02	0.439	1.1	0.02	0.489
Residual	91		0.9			0.9			0.9	
Total	96		1			1			1	

Note: Corresponding analyses of dispersion are shown in Appendix S1: Figure S6.

*S. mearnsi* (Bifidobacteriales), both of which may be associated with saccharolytic functions.

## DISCUSSION

Our study documented variation in the gut microbiomes of co-occurring and functionally distinct rodent species. In support of our first hypothesis, interspecific differences in microbiome composition were strong and consistent against the backdrop of rainfall-driven population size fluctuations (Figure 2). Unexpectedly, we found only partial support for our second hypothesis: increases in host population sizes were strongly and consistently associated with greater levels of microbiome diversity, but each host species differed in the degree to which this diversity was partitioned among individuals (Figure 3). We only found a significant positive correlation between individual-level microbiome richness and population size for *A. hindei*, despite observing significant positive correlations between overall microbiome richness and population size for all three host species (Figure 3). Because total microbiome diversity increased with population size without a concomitant increase in individual-level

microbiome diversity for both *G. robustus* (the generalist) and *S. mearnsi* (a specialist), these host species must have exhibited an increase in among-individual variation. The data also revealed evidence contrary to our third hypothesis, because neither of the specialist species (*A. hindei* and *S. mearnsi*) exhibited substantially different levels of spatiotemporal turnover in microbiome composition compared with the widespread generalist *G. robustus* (Figure 4; Tables 2 and 3; Appendix S1: Figure S6). Our community-level analysis thus revealed that microbiomes vary with respect to space and time for the three host species, but they varied in ways that did not align with the axes of dietary generalism and specialism or the changes in population density that have become so prominent as predictor variables in recent studies of host–microbiome interactions.

Whereas the phylogenetic relatedness of host species is generally strongly predictive of mammalian gut microbiome similarity at global scales (Mallott & Amato, 2021), we found substantially greater microbiome similarity between the two host species from different rodent families that exhibited overlapping isotopic dietary niches and site occupancies (*S. mearnsi*, Nesomyidae and *A. hindei*, Muridae) compared with the two confamilial



**TABLE 3** Permutational multivariate analysis of variance (PERMANOVA) testing the effects of population size, site, and the population size  $\times$  site interaction on Bray–Curtis dissimilarity of Phylogenetic Investigation of Communities by Reconstruction of Unobserved States (PICRUST)-predicted functional pathways.

Variable	df	Pseudo- <i>F</i>	<i>R</i> <sup>2</sup>	<i>p</i>
<i>Aethomys hindei</i>				
Population size	1	1.1	0.01	0.229
Site	2	1.7	0.03	0.060
Population size $\times$ site	2	0.8	0.01	0.666
Residual	99		0.94	
Total	104		1	
<i>Gerbilliscus robustus</i>				
Population size	1	0.6	0.01	0.640
Site	2	1.6	0.03	0.103
Population size $\times$ site	2	2.3	0.05	0.120
Residual	86		0.91	
Total	91		1	
<i>Saccostomus mearnsi</i>				
Population size	1	0.7	0.01	0.894
Site	2	3.2	0.06	0.004
Population size $\times$ site	2	1.1	0.02	0.267
Residual	91		0.91	
Total	96		1	

Note: Corresponding analyses of dispersion are shown in Appendix S1: Figure S6.

species with divergent ecologies (*G. robustus* and *A. hindei*, both Muridae; Brown et al., 2023). Yet, despite observing significant spatiotemporal differences in overall microbiome richness and composition for all three host species, we did not find overwhelming evidence that the underlying similarity of host microbiomes generally promotes a qualitatively similar response of the microbiome to ecological changes through space and time. Commonalities in the patterns that emerged from these host–microbiome interactions—such as consistently strong increases in population-level microbiome richness with population size and similarities between microbiomes of distantly related herbivores—occurred despite substantial differences in how bacterial diversity was distributed among host individuals.

The composition of an individual's microbiome represents a small slice of the total microbial diversity represented by the whole population. When the total microbial diversity of a population expands, host individuals may contribute to this expansion either by increasing their internal diversity in similar ways or by

exhibiting increasingly nonoverlapping gut microbiomes (Araújo et al., 2011). *G. robustus*, on average, occupied more plots, maintained a broader dietary niche, and exhibited less variable population sizes in response to rainfall compared with both *A. hindei* and *S. mearnsi*, but surprisingly its populations did not exhibit greater overall microbiome richness. Instead, *G. robustus* and the latter two host species exhibited similar total levels and rates of increase in population-level microbiome richness with population size, but only *A. hindei* exhibited enhanced individual-level microbiome richness in large and growing populations. This suggests that individual *A. hindei* microbiomes expanded in relatively similar ways as populations grew. By contrast, microbiomes of the two other host species did not exhibit a concomitant increase in individual-level richness with population size, suggesting that individuals occupied increasingly nonoverlapping niches in high-density populations and thus harbored increasingly unique fractions of the population's total diversity. Other studies of wild mammals have found increases in individual microbiome diversity during periods of resource abundance and nutritional quality that would contribute to population growth (Amato et al., 2015; Baniel et al., 2021; Ren et al., 2017), yet our comparative analyses suggest that there may not generally be a monotonic relationship between individual- and population-level diversity as populations grow. The extent to which individualistic responses contribute to the total niche width of populations has been a topic of significant interest in recent studies of resource use (Tinker et al., 2012), habitat occupancy (Newsome et al., 2015), and animal movement (Hertel et al., 2020)—similar investigations of how total microbiome diversity is partitioned among individuals could contribute to a more general understanding of how microbiome diversity is established and maintained in wildlife populations as well.

Comparisons of bacterial taxonomic, phylogenetic, and predicted functional composition can reveal functional redundancy within and among microbiomes. Our data revealed variation in the taxonomic richness and composition of microbiomes with relatively little concomitant variation in the predicted functional pathways associated with each microbiome (Figures 2–4; Tables 2 and 3; Appendix S1: Figure S5). This suggests microbiomes exhibited functional redundancy that may have enabled hosts to maintain similar physiological processes in their digestive tracts when turnover in bacterial taxa occurred (Moya & Ferrer, 2016). Some of this consistency may have arisen from functions attributed to the two predominant phyla (Firmicutes and Bacteroidetes; Figure 2E,F; Appendix S1: Figure S4), despite the finer grained differences in bacterial taxa associated with each

host species (Figure 2A–D). Quantifying and comparing bacterial predicted functions may therefore provide insight into the ways that compositionally distinct microbiomes contribute to the performance of hosts that occupy different niches. A striking example involves the enrichment of predicted pathways associated with degrading aromatic compounds in the microbiomes of *S. mearnsi* compared with both *A. hindei* and *G. robustus* (Appendix S1: Figure S5). The number of top predicted pathways associated with aromatic compounds in *S. mearnsi* suggests it may process higher quantities of lignin or other plant chemical defenses in its diet (Appendix S1: Figure S6; Prajapati et al., 2016), which would be consistent with its preference for chemically defended forbs in rainy seasons (Metz & Keesing, 2001). Although the two herbivorous species occupied virtually identical isotopic niches (Figure 1; Brown et al., 2023), elucidating differences in the diversity of plant taxa and their chemical defenses could help illuminate causal drivers of variation in host–microbiome associations. Metagenomic strategies to measure fine-grained functional genetic variation both within and among individual microbiomes—and to evaluate functional diet–microbiome linkages—could help establish the extent of functional redundancy within these taxonomically diverse gut microbiomes.

A contrast between the general tendency of larger host populations to harbor greater microbiome diversity and the idiosyncrasies involved with whether individual-level microbiomes diversify in large populations highlights a need to elucidate the mechanisms underlying this variation in wild mammals. Our comparison of three rodent species in a common environment suggests differences in the sensitivities of individual diets, demographic parameters, and/or microbial predicted functionality to variation in the host's local environment. Metagenomics studies that do not simply make predictions about the functions that bacteria perform for hosts based on bacterial taxonomy, but that instead directly quantify the functional genetic diversity within bacterial communities, could further elucidate factors that modulate microbiome composition in natural systems. Clearly, though, our comparative study shows a general pattern of seasonal loss and recovery of microbiome diversity in response to sources of environmental variation that cause diverse host populations in the wild to shrink and grow again.

## AUTHOR CONTRIBUTIONS

Bianca R. P. Brown and Tyler R. Kartzinel designed the study and conducted DNA analyses. Bianca R. P. Brown, Tyler R. Kartzinel, Jacob R. Goheen, Robert M. Pringle, Rhiannon P. Jakopak, Courtney G. Reed, Marissa Dyck, Alois Wambua, and Leo M. Khasoha conducted

fieldwork. Jacob R. Goheen, Robert M. Pringle, and Todd M. Palmer established the study plots. Seth D. Newsome led isotope data analysis. Bianca R. P. Brown and Tyler R. Kartzinel analyzed the data and wrote the initial manuscript, with contributions from all the authors.

## ACKNOWLEDGMENTS

We thank the Government of Kenya and Mpala Research Centre for permission to conduct this research. We are grateful for the field assistance by Gilbert Busienei and Deborah Boro.

## FUNDING INFORMATION

An NSF Graduate Research Fellowship, Institute at Brown for Environment and Society Graduate Research Training Grant, and a Department of Ecology, Evolution and Organismal Biology Doctoral Dissertation Enhancement Grant from the Bushnell Graduate Research and Education Fund to Bianca R. P. Brown; NSF DEB-1930820 and DEB-2026294 to Tyler R. Kartzinel; NSF DEB-1656527 to Robert M. Pringle; NSF DEB-1547679, DEB-1930763, DEB-2018405, DEB-2132265, NSERC Research Tools and Instruments grant, and the University of Wyoming to Jacob R. Goheen.

## CONFLICT OF INTEREST STATEMENT

The authors declare no conflicts of interest.

## DATA AVAILABILITY STATEMENT

Illumina 16S rRNA data are available from the National Center for Biotechnology Information (NCBI) Sequence Read Archive (SRA): BioProject PRJNA961814; <https://www.ncbi.nlm.nih.gov/bioproject/?term=PRJNA961814>. All data tables (Brown et al., 2024) are available from Dryad: <https://doi.org/10.5061/dryad.vx0k6djz3>.

## ORCID

Bianca R. P. Brown  <https://orcid.org/0000-0002-3110-5708>

Courtney G. Reed  <https://orcid.org/0000-0003-1083-3009>

Robert M. Pringle  <https://orcid.org/0000-0001-7487-5393>

## REFERENCES

- Alberdi, A., O. Aizpurua, K. Bohmann, M. L. Zepeda-Mendoza, and M. T. P. Gilbert. 2016. "Do Vertebrate Gut Metagenomes Confer Rapid Ecological Adaptation?" *Trends in Ecology & Evolution* 31: 689–699.
- Alston, J. M., C. G. Reed, L. M. Khasoha, B. R. P. Brown, G. Busienei, N. Carlson, T. C. Coverdale, et al. 2022. "Ecological Consequences of Large Herbivore Exclusion in an African Savanna: 12 Years of Data from the UHURU Experiment." *Ecology* 103: e3649.

- Amato, K. R., S. R. Leigh, A. Kent, R. I. Mackie, C. J. Yeoman, R. M. Stumpf, B. A. Wilson, K. E. Nelson, B. A. White, and P. A. Garber. 2015. "The Gut Microbiota Appears to Compensate for Seasonal Diet Variation in the Wild Black Howler Monkey (*Alouatta pigra*)."  
*Microbial Ecology* 69: 434–443.
- Anderson, M. J., and D. C. I. Walsh. 2013. "PERMANOVA, ANOSIM, and the Mantel Test in the Face of Heterogeneous Dispersions: What Null Hypothesis Are You Testing?"  
*Ecological Monographs* 83: 557–574.
- Araújo, M. S., D. I. Bolnick, and C. A. Layman. 2011. "The Ecological Causes of Individual Specialisation." *Ecology Letters* 14: 948–958.
- Baniel, A., K. R. Amato, J. C. Beehner, T. J. Bergman, A. Mercer, R. F. Perlman, L. Petrullo, et al. 2021. "Seasonal Shifts in the Gut Microbiome Indicate Plastic Responses to Diet in Wild Geladas." *Microbiome* 9: 26.
- Douglas Bates, M. M., B. Bolker, and S. Walker. 2015. "Fitting Linear Mixed-Effects Models Using lme4." *Journal of Statistical Software* 67: 1548–7660.
- Björk, J. R., M. R. Dasari, K. Roche, L. Grieneisen, T. J. Gould, J.-C. Grenier, V. Yotova, et al. 2022. "Synchrony and Idiosyncrasy in the Gut Microbiome of Wild Baboons." *Nature Ecology & Evolution* 6: 955–964.
- Bokulich, N. A., B. D. Kaehler, J. R. Rideout, M. Dillon, E. Bolyen, R. Knight, G. A. Huttley, and J. Gregory Caporaso. 2018. "Optimizing Taxonomic Classification of Marker-Gene Amplicon Sequences with QIIME 2's q2-Feature-Classifer Plugin." *Microbiome* 6: 90.
- Brown, B. R. P., J. R. Goheen, S. D. Newsome, R. M. Pringle, T. M. Palmer, L. M. Khasoha, and T. R. Kartzinell. 2023. "Host Phylogeny and Functional Traits Differentiate Gut Microbiomes in a Diverse Natural Community of Small Mammals." *Molecular Ecology* 32: 2320–34.
- Brown, B. R. P., L. M. Khasoha, P. Lokeny, R. P. Jakopak, C. G. Reed, M. A. Dyck, A. Wambua, et al. 2024. "Spatiotemporal Variation in the Gut Microbiomes of Co-Occurring Wild Rodent Species." Dataset. Dryad. <https://doi.org/10.5061/dryad.vx0k6djz3>.
- Brown, J. H. 1984. "On the Relationship between Abundance and Distribution of Species." *The American Naturalist* 124: 255–279.
- Callahan, B. J., P. J. McMurdie, M. J. Rosen, A. W. Han, A. J. A. Johnson, and S. P. Holmes. 2016. "DADA2: High-Resolution Sample Inference from Illumina Amplicon Data." *Nature Methods* 13: 581–83.
- Douglas, G. M., V. J. Maffei, J. R. Zaneveld, S. N. Yurgel, J. R. Brown, C. M. Taylor, C. Huttenhower, and M. G. I. Langille. 2020. "PICRUSt2 for Prediction of Metagenome Functions." *Nature Biotechnology* 38: 685–88.
- Goheen, J. R., D. J. Augustine, K. E. Veblen, D. M. Kimuyu, T. M. Palmer, L. M. Porensky, R. M. Pringle, et al. 2018. "Conservation Lessons from Large-Mammal Manipulations in East African Savannas: The KLEE, UHURU, and GLADE Experiments." *Annals of the New York Academy of Sciences* 1429: 31–49.
- Goheen, J. R., T. M. Palmer, G. K. Charles, K. M. Helgen, S. N. Kinyua, J. E. Maclean, B. L. Turner, H. S. Young, and R. M. Pringle. 2013. "Piecewise Disassembly of a Large-Herbivore Community across a Rainfall Gradient: The UHURU Experiment." *PLoS One* 8: e55192.
- Hertel, A. G., P. T. Niemelä, N. J. Dingemanse, and T. Mueller. 2020. "A Guide for Studying among-Individual Behavioral Variation from Movement Data in the Wild." *Movement Ecology* 8: 30.
- Hsieh, T. C., K. H. Ma, and A. Chao. 2016. "iNEXT: An R Package for Rarefaction and Extrapolation of Species Diversity (Hill Numbers)." *Methods in Ecology and Evolution* 7: 1451–56.
- Jesmer, B. R., M. J. Kauffman, M. A. Murphy, and J. R. Goheen. 2020. "A Test of the Niche Variation Hypothesis in a Ruminant Herbivore." *Journal of Animal Ecology* 89: 2825–39.
- Kartzinell, T. R., J. R. Goheen, G. K. Charles, E. DeFranco, J. E. MacLean, T. O. Otieno, T. M. Palmer, and R. M. Pringle. 2014. "Plant and Small-Mammal Responses to Large-Herbivore Exclusion in an African Savanna: Five Years of the UHURU Experiment." *Ecology* 95: 787.
- Kartzinell, T. R., J. C. Hsing, P. M. Musili, B. R. P. Brown, and R. M. Pringle. 2019. "Covariation of Diet and Gut Microbiome in African Megafauna." *Proceedings of the National Academy of Sciences of the United States of America* 116: 23588–93.
- Katoh, K. 2002. "MAFFT: A Novel Method for Rapid Multiple Sequence Alignment Based on Fast Fourier Transform." *Nucleic Acids Research* 30: 3059–66.
- Kernaléguen, L., J. P. Y. Arnould, C. Guinet, and Y. Cherel. 2015. "Determinants of Individual Foraging Specialization in Large Marine Vertebrates, the Antarctic and Subantarctic Fur Seals." *Journal of Animal Ecology* 84: 1081–91.
- Laake, J. L. 2013. *RMark: An R Interface for Analysis of Capture-Recapture Data with MARK*. Seattle, WA: U.S. Department of Commerce, National Oceanic and Atmospheric Administration, National Marine Fisheries Service, Alaska Fisheries Science Center.
- Levins, R. A. 1969. "Some Demographic and Genetic Consequences of Environmental Heterogeneity for Biological Control." *Bulletin of the Entomological Society of America* 15: 237–240.
- Mallott, E. K., and K. R. Amato. 2021. "Host Specificity of the Gut Microbiome." *Nature Reviews. Microbiology* 19: 639–653.
- Martinez Arbizu, P. 2017. "pairwiseAdonis: Pairwise Multilevel Comparison Using Adonis." <https://github.com/pmartinezarbizu/pairwiseAdonis>.
- Maurice, C. F., S. C. Knowles, J. Ladau, K. S. Pollard, A. Fenton, A. B. Pedersen, and P. J. Turnbaugh. 2015. "Marked Seasonal Variation in the Wild Mouse Gut Microbiota." *The ISME Journal* 9: 2423–34.
- Metz, M. R., and F. Keesing. 2001. "Dietary Choices of the Pouched Mouse (*Saccostomus mearnsi*) in Central Kenya." *Biotropica* 33: 182–87.
- Morton, J. T., C. Marotz, A. Washburne, J. Silverman, L. S. Zaramela, A. Edlund, K. Zengler, and R. Knight. 2019. "Establishing Microbial Composition Measurement Standards with Reference Frames." *Nature Communications* 10: 2719.
- Moya, A., and M. Ferrer. 2016. "Functional Redundancy-Induced Stability of Gut Microbiota Subjected to Disturbance." *Trends in Microbiology* 24: 402–413.
- Newsome, S. D., H. M. Garbe, E. C. Wilson, and S. D. Gehrt. 2015. "Individual Variation in Anthropogenic Resource Use in an Urban Carnivore." *Oecologia* 178: 115–128.

- Oksanen, J., F. G. Blanchet, M. Friendly, R. Kindt, P. Legendre, D. McGlinn, P. R. Minchin, et al. 2017. "Package 'Vegan'." R Package Ver. 2.0-8. 254 pp.
- Prajapati, V. S., H. J. Purohit, D. V. Raje, N. Parmar, A. B. Patel, O. A. H. Jones, and C. G. Joshi. 2016. "The Effect of a High-Roughage Diet on the Metabolism of Aromatic Compounds by Rumen Microbes: A Metagenomic Study Using Mehsani Buffalo (*Bubalus bubalis*)."  
*Applied Microbiology and Biotechnology* 100: 1319–31.
- Price, M. N., P. S. Dehal, and A. P. Arkin. 2009. "FastTree: Computing Large Minimum Evolution Trees with Profiles Instead of a Distance Matrix."  
*Molecular Biology and Evolution* 26: 1641–50.
- Quast, C., E. Pruesse, P. Yilmaz, J. Gerken, T. Schweer, P. Yarza, J. Peplies, and F. O. Glöckner. 2013. "The SILVA Ribosomal RNA Gene Database Project: Improved Data Processing and Web-Based Tools."  
*Nucleic Acids Research* 41: D590–D596.
- R Development Core Team. 2021. *R: A Language and Environment for Statistical Computing*. Vienna: R Foundation for Statistical Computing.
- Reese, A. T., and R. R. Dunn. 2018. "Drivers of Microbiome Biodiversity: A Review of General Rules, Feces, and Ignorance."  
*MBio* 9: e01294-18.
- Ren, T., S. Boutin, D. Coltman, M. Humphries, B. Dantzer, J. Gorrell, A. McAdam, and M. Wu. 2017. "Seasonal, Spatial, and Maternal Effects on Gut Microbiome in Wild Red Squirrels."  
*Microbiome* 5: 163.
- Sharpton, T. J. 2018. "Role of the Gut Microbiome in Vertebrate Evolution."  
*MSystems* 3: e00174-17.
- Shipley, L. A., J. S. Forbey, and B. D. Moore. 2009. "Revisiting the Dietary Niche: When Is a Mammalian Herbivore a Specialist?"  
*Integrative and Comparative Biology* 49: 274–290.
- Thompson, L. R., J. G. Sanders, D. McDonald, A. Amir, J. Ladau, K. J. Locey, R. J. Prill, et al. 2017. "A Communal Catalogue Reveals Earth's Multiscale Microbial Diversity."  
*Nature* 551: 457–463.
- Tinker, M. T., P. R. Guimaraes, M. Novak, F. M. D. Marquitti, J. L. Bodkin, M. Staedler, G. Bentall, and J. A. Estes. 2012. "Structure and Mechanism of Diet Specialisation: Testing Models of Individual Variation in Resource Use with Sea Otters."  
*Ecology Letters* 15: 475–483.
- Trevelline, B. K., S. S. Fontaine, B. K. Hartup, and K. D. Kohl. 2019. "Conservation Biology Needs a Microbial Renaissance: A Call for the Consideration of Host-Associated Microbiota in Wildlife Management Practices."  
*Proceedings of the Biological Sciences* 286: 20182448.
- Trevelline, B. K., and K. D. Kohl. 2022. "The Gut Microbiome Influences Host Diet Selection Behavior."  
*Proceedings of the National Academy of Sciences of the United States of America* 119: e2117537119.
- Van Valen, L. 1965. "Morphological Variation and Width of Ecological Niche."  
*The American Naturalist* 99: 377–390.
- Voolstra, C. R., and M. Ziegler. 2020. "Adapting with Microbial Help: Microbiome Flexibility Facilitates Rapid Responses to Environmental Change."  
*BioEssays* 42: 2000004.
- Walters, W., E. R. Hyde, D. Berg-Lyons, G. Ackermann, G. Humphrey, A. Parada, J. A. Gilbert, et al. 2016. "Improved Bacterial 16S rRNA Gene (V4 and V4-5) and Fungal Internal Transcribed Spacer Marker Gene Primers for Microbial Community Surveys."  
*mSystems* 1: e00009–e00015.

## SUPPORTING INFORMATION

Additional supporting information can be found online in the Supporting Information section at the end of this article.

**How to cite this article:** Brown, Bianca R. P., Leo M. Khasoha, Peter Lokeny, Rhiannon P. Jakopak, Courtney G. Reed, Marissa Dyck, Alois Wambua, et al. 2024. "Spatiotemporal Variation in the Gut Microbiomes of Co-Occurring Wild Rodent Species."  
*Ecosphere* 15(5): e4854. <https://doi.org/10.1002/ecs2.4854>